Determining Stable Spans of Undercut Cemented Paste Backfill

M. Grabinsky, M. Jafari
University of Toronto, Toronto, Ontario, Canada

GEOQuébec 2015
Challenges from North to South
Des défis du Nord au Sud

ABSTRACT
A significant underground mine design challenge is predicting the stability of a previously placed cemented backfill when it is to be undercut in a subsequent stage of mining. Mitchell (1991) proposed several limit equilibrium analyses for this design situation based on different assumed modes of failure, but little has been done since then to more carefully consider the most appropriate means analysis approach. This paper considers a tentative framework for an alternate limit equilibrium solution, based on the assumption that the cemented backfill behaves as rigid struts to support the overlying fill. The advantage of this analysis approach is that it provides a unifying model for the previous disparate analysis methods. Remaining challenges to using this analysis for practical design will be addressed.

RÉSUMÉ
Un défi de conception important de mine souterraine est de prédire la stabilité d'un remblai cimenté placé dans le passé, quand il doit être rongé lors d'une étape ultérieur de l'exploitation minière. Mitchell (1991) a proposé plusieurs analyses d'équilibre limite, pour cette situation de conception, basées sur différents modes hypothétiques de rupture, mais il y a eu peu d'avancée depuis pour examiner plus attentivement l'approche d'analyse la plus appropriée. Cet article considère un cadre provisoire pour une solution d'équilibre limite basée sur l'hypothèse que le remblai cimenté se comporte comme des supports rigides pour soutenir la couche de remblai qui le recouvre. L'avantage de cette approche d'analyse est qu'elle fournit un modèle unificateur pour les méthodes d'analyse disparates précédentes. Les défis restants de l'utilisation de cette analyse pour la conception seront abordés dans cet article.

1 INTRODUCTION

In underground mining it is often the case that a previously placed cemented backfill needs to be undercut in a subsequent mining stage. The previously placed cemented backfill, sometimes called a sill mat, is typically placed with a higher binder content and possibly some reinforcement, however their design was largely empirical until Mitchell and Roettger (1989) and Mitchell (1991) used a series of centrifugal physical model results to suggest some limit equilibrium solutions to assess different failure modes.

The authors are aware of major mining companies that continue to use Mitchell's 1991 solutions, and these same solutions have also been considered by others when designing rehabilitation strategies for old mine workings (Beauchamp et al.). Several authors refer to Mitchell's 1989 and/or 1991 works only to indicate it is a method available for one of the important underground mine design situations, without critical assessment. De Souza and Dirige (2001) have continued to use centrifuge modeling for underground backfilling problems but their results do not appear to have been applied widely. Importantly, no mining companies (or their consultants) appear to have published case studies comparing as-designed sill pillars with their actual field performance. To address this situation, Pakalnis and co-workers at the University of British Columbia, with their industry partners undertook an extensive field investigation of sill pillar performance at operating mines, using Mitchell's solutions for back-analysis and comparison with field observations (Pakalnis et al., 2005). Comparisons were also made between Mitchell's indicated failure modes and results of numerical analyses using FLAC2D (Doerner, 2005) although alternative failure modes were not assessed.

The scope of this paper is limited to (sub-)vertical stopes with unreinforced sill mats, which involves only the first three of Mitchell's limit equilibrium solutions (the fourth being relevant to backfills in shallow-dipping stopes). The failure modes considered by these limit equilibrium solutions involve i) failure of the exposed undercut fill due to tensile detachment; ii) beam bending failure; and iii) side shear block failure along the backfill-host rock interface and subsequent rigid block sliding. The basis for Mitchell's three limit equilibrium solutions is reviewed and some limitations are discussed. An alternative failure mode is then proposed which is motivated by the "strut and tie" model used as the basis for one of the reinforced concrete beam design methods. It has the advantage of unifying the three previous failure modes which were treated as separate mechanisms by Mitchell. Comparisons will be made with numerical models, and a path forward towards a rational design process is suggested.

2 REVIEW OF MITCHELL'S (1991) SOLUTIONS

Mitchell (1991) originally considered sill matt design in a very general way, including vertical to shallow-dipping backfilled stopes, and both reinforced and unreinforced sill mats. Here, the scope will be restricted to (sub-vertical) unreinforced sill mats.

The sill mat is generally loaded on its top surface by the overlying fill, which may or may not be cemented. Mitchell proposed assessing the surface load due to the overlying fill using the solution derived from an arching analysis,

$$\sigma_v = \gamma L / (2 K \tan\phi) \qquad [1]$$

Where σ_v is the vertical stress, γ is the backfilll unit weight, L is the horizontal length of the stope (hangingwall to footwall), K is the coefficient of lateral earth pressure, and ϕ is the angle of internal friction. This assumes the backfill does not develop pore water pressures and a total stress analysis is carried out. Mitchell suggests that it is "often assumed" $K = 1$; however lower values of K will increase the predicted σ_v. Alternatively, in some cases the stress path during filling does not correspond to the assumptions behind traditional arching analyses and the resulting imposed vertical stress can be lower than that suggested by Eq. [1] (Thompson et al., 2012). It must therefore be recognized that reliable prediction of σ_v is non-trivial.

2.1 Tensile Detachment

When the sill mat is undercut, the newly exposed underside becomes traction free and this will result in backfill stress relaxation in proximity. In the field this frequently results in observed "caving" of the backfill up to a point where the material tensile strength is equal to the resulting stresses. Mitchell suggested modeling the caved region as semi-circular; however, it should be recognized that this is a more extreme geometry than observed in the field.

The limit equilibrium solution is established by consider the driving force (downward) to be the self-weight of the failed caved region, and the resisting force (upward) to be the tensile strength integrated along the horizontal projected area of the failed surface. Thus the resisting force *Fr* will always be equal to $\sigma_t L$ where σ_t is the tensile strength. The larger the assumed area of the failed caved region, the more critical the tensile detachment mode of failure will become, and thus Mitchell's assumed semi-circular geometry probably over-predicts the required tensile strength in most cases. For the assumed semi-circular geometry the driving force *Fd* is equal to $½ \pi (½L)^2 \gamma = (\pi L^2 \gamma)/8$. Equating driving and resisting forces and rearranging produces Mitchell's expression (equation 3 in the original paper)

$$L \gamma > 8 \sigma_t / \pi \qquad [2]$$

Practicing engineers prefer to use the Unconfined Compressive Strength (UCS) as a reference strength, as well as an appropriate Strength Factor SF. Furthermore, it is common to assume σ_t = UCS/10 for geologic materials. Therefore, further rearrangement of the above equations results in a more convenient expression for design,

$$\text{UCS} = \text{SF}\ 4 L \gamma \qquad [3]$$

When using these equations it must be borne in mind that a semicircular geometry is assumed, which then imposes the geometric constraint:

$$d > ½ L \qquad [4]$$

where d is the sill mat depth.

2.2 Flexural Failure

For a fixed-ended beam under uniformly distributed load w, the maximum bending moment occurs at the ends and is equal to (according to Euler-Bernoulli beam theory) $w L^2 / 12$, and the maximum fiber stress is $w L^2 / 12Z$, where for a solid rectangular section $Z = b d^2 / 6$. For a two-dimensional analysis the depth into the plane can be taken as $b = 1$ and therefore the maximum fiber stress is $½ w (L/d)^2$. Given that cemented geomaterials are weaker in tension than in compression it is necessary that the tensile strength σ_t be at least equal to this maximum fiber stress and therefore $\sigma_t \geq ½ w (L/d)^2$. If a compressive confining stress σ_c acts across the length of the beam then this reduces the maximum fiber stress so that it can be written $\sigma_t \geq ½ w (L/d)^2 - \sigma_c$. Therefore, for a desired Strength Factor SF,

$$\sigma_t = \text{SF} (½ w (L/d)^2 - \sigma_c) \qquad [5]$$

Setting SF = 1, this can be rearranged to obtain Mitchell's expression $(L/d)^2 > 2(\sigma_t + \sigma_c)/w$ (equation 2 in the original paper). Here the distributed load w includes both applied loads σ_v as well as the self-weight effect γd. It should be noted that this is based on Euler-Bernoulli beam theory, i.e. that "plane sections remain plane" and this condition is increasingly inappropriate as the ratio L/d decreases (as the beam becomes thicker), which is probably the case for most sill mats. As well, predicting reasonable values of σ_c is also a non-trivial task, similar to σ_v.

Again assuming σ_t = UCS/10, the above equations can be rearranged to a form more suited to practical application,

$$\text{UCS} = \text{SF} (5 w (L/d)^2 - \sigma_c) \qquad [6]$$

It is conservative to assume that $\sigma_c = 0$ in which case UCS = SF 5 $w (L/d)^2$. Again it must be borne in mind that the usual Euler-Bernoulli beam theory assumptions are not valid for most sill mats, and that the assessments of w (σ_v) and σ_c are non-trivial. Most importantly, the equations are predicated on preventing the maximum fiber stress at the bottom of the sill mat from exceeding the backfill tensile strength; however, it is well known that for a fixed-ended beam this stress level will be well below the level eventually required to create plastic hinges in the beam and bring it to its ultimate condition. Therefore, even if all other assumptions are satisfied for the design conditions considered, the values given by equation [6] will be conservative.

2.3 Side Shear Block Failure

Similar to caving, this mode is assumed to be only potentially significant for thick sub-vertical sill mats. Taking the dip angle as β, the driving force $Fd \sin\beta$ along the sidewall direction is due to the vertical stress acting on the top surface, $\sigma_v L$, as well as the sill self-weight, $L\,d\,\gamma$, such that $Fd = L\,(\sigma_v + d\,\gamma)$. The shear force mobilized on the backfill-wall contacts is τ_f and acts over length $d/\sin\beta$ so that $Fr = \tau_f\, d / \sin\beta$. In the direction of the sidewall the equilibrium equation can be written $Fd \sin\beta = 2\, Fr$, and incorporating the engineering strength factor and making the substitutions for Fd and Fr this becomes

$$\mathrm{SF}\, L\,(\sigma_v + d\,\gamma) \sin\beta = 2\,\tau_f\, d / \sin\beta \qquad [7]$$

Setting SF =1, this can be rearranged to obtain Mitchell's expression $(\sigma_v + d\,\gamma) > 2\,(\tau_f / \sin^2\beta)\,(d/L)$ (equation 4 in the original paper). Mitchell and Wong (1982) and Mitchell et al. (1982) show that for small strains the shear strength at initial yield is $\tau_f = ½$ UCS. Substituting this into equation [7] and rearranging, it can conservatively be written

$$\mathrm{UCS} = \mathrm{SF}\, L\,(\sigma_v / d + \gamma) \sin^2\beta \qquad [8]$$

It should be noted that equations [3], [6] and [8] are extensions of Mitchell's original equations and have incorporated some commonly assumed relationships between different strength parameters for geomaterials, however the advantage of using the equations in these forms is that it allows a common basis for comparing required backfill UCS required to resist tensile detachment (caving), flexure, a side shear block failure modes, respectively, and to thereby determine which mode is critical in design. All of the previously noted limitations should be borne in mind when using these equations, and it must be remembered that the failure modes were derived from independently assessed failure mechanisms. In the following section a unifying model is presented that attempts to integrate the analysis of these modes.

3 PROPOSED ALTERNATE MODEL

In the design of reinforced concrete beams one method of analysis that can be used is the "strut-and-tie" model in which the steel reinforcement simulates ties that can carry tensile stresses and the (plain) concrete simulates struts that carry compressive stresses. For an unreinforced sill mat this can be simplified to simply a strut model. The basis for this model in assessing sill mat stability is shown in Figure 1. In general, it is assumed that the sill mat can be analysed as consisting of two internal symmetric trapezoidal sections that react against the hostrock at either side (the "abutments"), and against each other in the middle. The generation of horizontal reaction forces at the abutments allows for a corresponding vertical shear reaction which resists the vertical stress imposed by overlying backfill. No shear exists on the mid-plane (the contact between the two struts) due to the symmetry at this location. The offset between the horizontal reaction forces imposes a moment which resists the moment generated by the overlying fill.

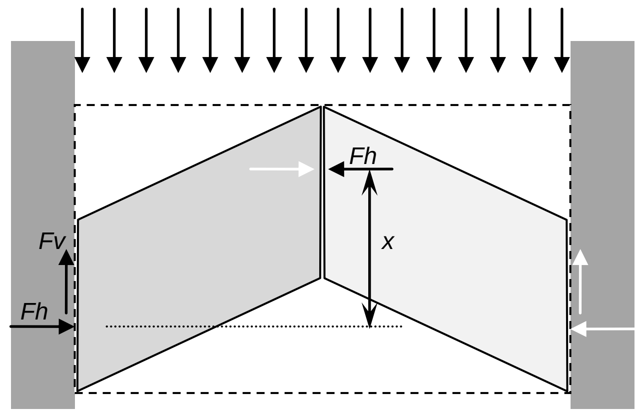

Figure 1. Assumed model for sill mat stability assessment

The force components can be assessed by isolating one of the struts and examining its free body diagram. For vertical equilibrium $Fv = ½\, L\,(\sigma_v + d\,\gamma)$ and for moment equilibrium (e.g., taking moments about any point along the sidewall) $Fh = ¼\, L^2\,(\sigma_v + d\,\gamma) / x$. To determine x, assumptions could be made about the thickness of the struts and the shape of the stress distributions on each face; instead, numerical analysis will be used in the next section to guide the most appropriate assumptions. As will be discussed, for real design situations it is likely necessary to carry out numerical analysis to assess the geometric limits of the detailed design under consideration; once the appropriate geometry/geometries have been defined, limit equilibrium equations can subsequently be carried out for routine designs to determine the appropriate backfill UCS requirements.

The potential for tensile detachment is significantly less than Mitchell's assumed semi-circular geometry. In real design situations more detailed measures, likely incorporating reinforcement, would have to be used if the underlying excavation was re-entry (i.e., if personnel were to go back in). Thus the assumed unreinforced mat is appropriate for non-re-entry situations. The tensile detachment calculation can be undertaken once the strut geometry is determined from numerical analysis, but in practice it is normally assumed that minor caving will occur and care must be taken to avoid re-excavating this spoil material in the subsequent stage of stope extraction.

The flexural failure mechanism is drastically different than Mitchell's assumed critical mode. Here, once the left and right stress distributions corresponding to Fh are determined, the maximum compressive stress can be compared to the UCS to ensure backfill crushing does not occur.

The side shear block failure mechanism will be identical to the Mitchell analysis. It should be noted that for large open stopes the production blasting typically results in very rough wall surfaces and so shear through the weaker backfill material should be expected in these situations. As a result, the full backfill internal shear strength may be used.

4 EXAMPLE NUMERICAL ANALYSIS

The following analysis shows how numerical results can be used to guide the detailed development of the generalized model presented in the previous section. Once this has been done, simplified limiting equilibrium solutions can be developed so that practicing engineers can quickly carry out routine design calculations, without further aid of numerical analysis.

The example considers a sill mat L = 10 m wide and d = 6 m deep. The host rock is assumed elastic with Young's Modulus 70 GPa. The backfill in the sill mat is considered elastic-perfectly plastic with Young's Modulus 5 GPa, unit weight γ = 20 kN/m^3, and Mohr-Coulomb strength parameters cohesion c = ¼ UCS, internal friction angle ϕ = 37°, and tensile strength σ_t = UCS/10. (The parameterized cohesion is appropriate to the chosen ϕ.) The tensile strength is reduced to zero once exceeded, and no dilation is assumed during plastic shearing. The contacts have a similar strength model as the backfill.

Contact stiffness must be selected carefully for such analyses. Here, the contact is not comprised of two distinct rock surfaces filled with gouge of nominal thickness and known mechanical properties. Instead, it is assumed that the contact represents the effects of non-uniform filling between the backfill and host rock and that this would only occur on the mm-scale. Thus, the analyses are checked for contact displacements and the contact stiffness adjusted so that the predicted displacements remain in the mm-range.

The geometry of the initial model is shown in Figure 2. For an assumed UCS = 5 MPa and applied σ_v = 100 kPa the response is essentially elastic. Figure 3 shows the stress trajectories (with long axis oriented in the direction of major compressive stress) and indicates that significant arching is occurring between the two abutments. However, the effect of the stress reduction due to undercutting is also evident with only the top half of the mat retaining a minimum principle stress that is still compressive.

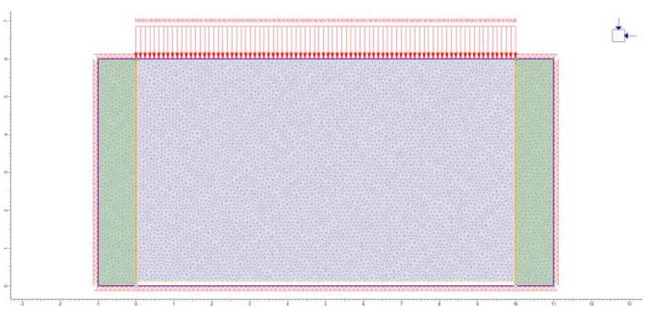

Figure 2. Geometry of initial model.

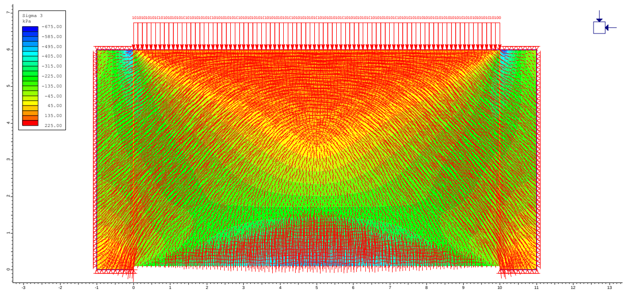

Figure 3. Stress trajectories and minimum principle stresses at 100 kPa load level

Increasing σ_v beyond this 100 kPa level results in the onset of convergence issues which arise from the onset of a potential caving mechanism. As previously indicated, for non-re-entry stoping this failure mechanism can be handled and so this does not really represent the critical design.

To better simulate the subsequent strut-type behaviour of the sill mat an alternate model, shown below, is generated that is motivated by the mechanism shown in Figure 1 and stress results shown in Figure 3. In this figure the vertical applied stress σ_v has been increased to 250 kPa.

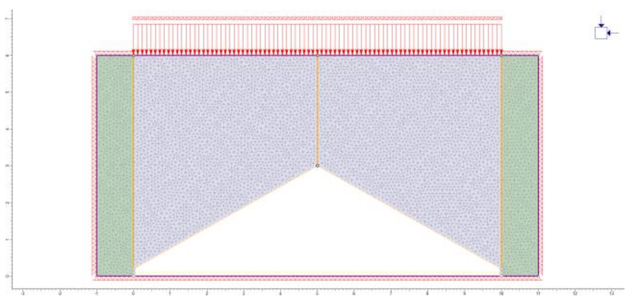

Figure 4. Geometry of modified strut model

At this load level the maximum compressive stress at the top mid-span of the matt is 880 kPa, still well below the 5 MPa modeled UCS, and Figure 5 shows good evidence of arching action through the modeled struts. In fact, the most critical area for compressive strength is at about mid-height of the abutment (Figure 6) where the modeled SF is still about 2.0 for the assumed 250 kPa σ_v.

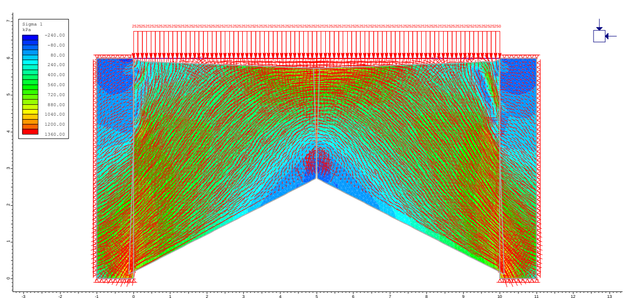

Figure 5. Stress trajectories and maximum principle stresses at 250 kPa load level

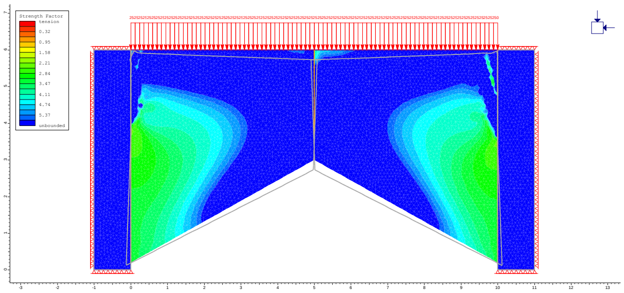

Figure 6. Strength Factors and deformed shape

To better understand the stress distributions acting on the contact surfaces the following figures are considered. Figure 7 is the centerline contact. The shear stresses (not shown) are near zero as expected due to the symmetry consideration. The normal stress distribution is linear with tensile stress (still less than the modeled tensile strength) at the bottom and maximum compressive stress at the top.

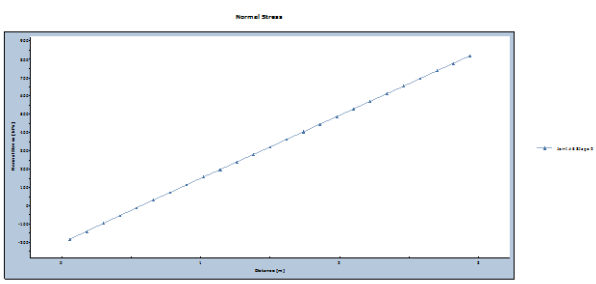

Figure 7. Linear normal stress distribution occurring at the mid-span vertical joint in the modeled sill mat

At the vertical abutment contact it appears that there has been some detachment or stress relaxation in the upper portion, such that only the lower two-thirds of the sill mat effective take compression and contribute to the modeled strut behaviour. Within this compressive zone, however, the normal stress distribution is linear (Figure 8). Also within this compressive zone the shear stresses are essentially constant (not shown) with magnitude about 400 kPa.

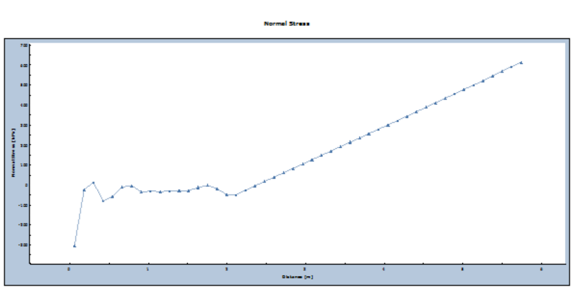

Figure 8. Linear normal stress distribution occurring at the abutment vertical joint

For horizontal equilibrium, the reaction at the abutment is roughly 300 kPa average normal stress acting over 4 m for a thrust of 1,200 kN (per m into plane of analysis); and the reaction at the mid-plane is roughly 400 kPa average normal stress acting over 4 m for a thrust of 1,200 kN, so horizontal equilibrium is satisfied. For vertical equilibrium, the reaction at the abutment is roughly 400 kPa constant shear stress acting over 4 m for a traction of 1,600 kN (per m into plane of analysis); the vertical force due to applied stress is 1,250 kN and the self-weight is 450 kN, so vertical equilibrium is satisfied (within the approximations used in these calculations). For moment equilibrium it is necessary to determine the locations of the horizontal thrusts and thus the distance between their lines of action (x in Figure 1). Both stress distributions are linear and therefore the resultants will act at the third-height from their maximum values. The horizontal thrust at the mid-plane then acts at about 1 m from the top of the sill mat, while the horizontal thrust at the abutment acts about 4.67 m from the top, such that x = 3.67 m. Therefore the resisting moment is 1,200 kN $\times$ 3.67 m = 4,400 kNm. The driving moment (about the abutment) is 3,125 kNm due to the applied vertical load, and 1,000 kNm due to self-weight, so moment equilibrium is satisfied (within the approximations used in these calculations). These results are summarized in Figure 9.

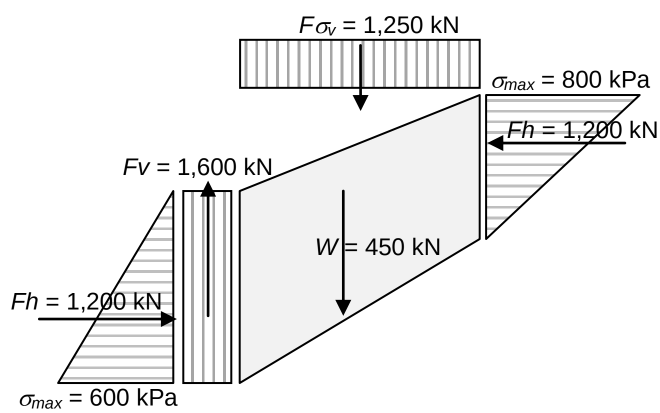

Figure 9. Summary of results approximated from the numerical analysis

Finally, as mentioned in the previous section, once the appropriate geometry has been identified it is possible to assess resistance needed to prevent the tensile detachment (caving) mechanism identified by Mitchell. Here, the driving force *Fd* would be calculated as the half-length $\times$ modeled height of cave $\times$ unit weight (per unit width) or 5 m $\times$ 3 m $\times$ 20 kN/m^3 = 300 kN/m. The required material strength would be UCS = 10 Fd / L = 300 kPa. This compares to 800 kPa using Equation [8] and a SF = 1. Thus the predicted stability against caving using the strut model, as well as the caving geometry, is more consistent with field observations.

5 CONCLUSIONS AND FUTURE WORK

This paper has presented only a single analysis in support of the proposed concept to illustrate the general model being employed and to highlight the approach towards developing more practical preliminary design tools for sill mats. Within the context of this preliminary investigation, the numerical analysis results support the notion that the strut model is a useful analogue for simulating the effect of an unreinforced sill mat that must support overlying backfill in a (sub-)vertical stope. It has the advantage that the strut analogue can be used create numerical models that more realistically simulate observed field behaviour of unreinforced sill mats, without running into spurious convergence problems caused by numerical issues in areas of the model that are not important to design (notably, in stress relaxation zones).

A great deal more work is required to determine how to better identify optimal strut geometry and thus generate the stress distributions and force resultants that can be used for limit equilibrium equations in the simplified strut design. However, once this is done, it has the potential to provide designers with practical and easy calculations to assess preliminary designs of unreinforced sill mats that are undercut by non-re-entry stopes.

ACKNOWLEDGEMENTS

This work was financially supported by Barrick Gold Corp. and the Natural Sciences and Engineering Research Council.

REFERENCES

Beauchamp, K.J., et al. "Addressing Mine Hazards under Transportation Corridors–The Timmins Experience." (https://www.dot.ny.gov/conferences/itgaum/repository/2F_Beauchamp_et_al_mine%20hazards_timmins%20experience.pdf, accessed 29-05-2015)

De Souza, E., and A. P. Dirige 2001. "Procedures for the design of sillmats with paste backfill." In DC Rocks 2001, The 38th US Symposium on Rock Mechanics (USRMS). American Rock Mechanics Association, 2001.

Doerner, C.A.C. 2005. Effect of Delayed Backfill in Open Stope Mining Methods. M.A.Sc. Thesis, University of British Columbia, Vancouver, Canada, 152 p.

Mitchell, R.J. 1991. Sill mat evaluation using centrifugal models. *Mining Science and Technology*, 13:301-313. (Note that the article appeared in the last issue of the journal; the journal was subsequently incorporated into Engineering Geology (0013-7952), also an Elsevier publication)

Mitchell, R.J. and Roettger, J.J. 1989. Analysis and modelling of sill pillars. Innovations in Mining Backfill Technology. Balkema, Rotterdam: 53-62.

Mitchell, R.J. and Wong, B.C. 1982. Behaviour of cemented tailings sands. Canadian Geotechnical Journal, 19:289-295.

Mitchell, R.J., Olsen, R.S. and Smith, J.D. 1982. Model studies on cemented tailings used in mine backfill. Canadian Geotechnical Journal, 19:14-28.

Pakalnis, R., Caceres, C., Clapp, K. and Morin, M. 2005. Design spans – underhand cut and fill mining. Proceedings of the 107th Annual General Meeting of the Canadian Institute of Mining (CIM-AGM), Toronto, April 2005, 9 pp.

Thompson, B.D., Bawden, W.F. and Grabinsky, M.W., 2012. “In-situ Measurements of Cemented Paste Backfill at the Cayeli Mine”, Canadian Geotechnical Journal, Vol. 49, No. 7, pp. 755-772.